Unravelling ethanol metabolic pathways under different feeding regimes in anaerobic digestion ecosystems

Title	Unravelling ethanol metabolic pathways under different feeding regimes in anaerobic digestion ecosystems
Author(s)	Chang, Huanhuan;Sun, Yuepeng;Liu, Tingxia;Wu, Guangxue
Publication Date	2025-04-18
Publisher	Elsevier

Journal of Environmental Chemical Engineering 13 (2025) 116688

Contents lists available at ScienceDirect

Journal of Environmental Chemical Engineering

journal homepage: www.elsevier.com/locate/jece

Unravelling ethanol metabolic pathways under different feeding regimes in anaerobic digestion ecosystems

Huanhuan Chang [a], Yuepeng Sun [b], Tingxia Liu [a], Guangxue Wu [a,*]

[a] Civil Engineering, School of Engineering, College of Science and Engineering, University of Galway, Galway H91 TK33, Ireland
[b] School of Ecology and Environment, Inner Mongolia University, Hohhot, Inner Mongolia 010021, China

ARTICLE INFO

Keywords:
Butyrate production
Ethanol metabolism
Feeding regimes
Interspecies electron transfer
Methanogenesis

ABSTRACT

Feeding regimes critically influence the efficiency of anaerobic digestion, yet its impact on ethanol-type anaerobic digestion ecosystems remains inadequately understood. A comprehensive investigation into the effect of feeding regimes on ethanol-type anaerobic digestion was conducted. Sequencing batch reactor (SBR) and continuous-flow reactor (CFR) were adopted for acclimating ethanol-type anaerobic methanogenesis. During long-term operation, the CFR system achieved complete removal of ethanol and volatile fatty acids, while an accumulation of 2250.0 ± 130.0 mg COD/L acetate and 931.0 ± 184.0 mg COD/L butyrate was observed in the SBR system. The difference was probably due to the limited activity of methanogens under acid accumulation conditions in SBR. Notably, the accumulation of acetate and the reduced pH in SBR facilitated ethanol metabolism towards butyrate production by a chain-elongating bacteria: *Clostridium*. Additionally, acetoclastic methanogenesis was not detected in SBR, and the dominated hydrogenotrophic methanogen was *Methanobacterium*. Ethanol was exclusively oxidized to acetate by ethanol oxidizers, including *Desulfolutivibrio* and *Desulfomicrobium*, facilitating interspecies hydrogen transfer with *Methanospirillum* in CFR. The electroactive bacteria *Geobacter* was enriched in CFR. Moreover, the relative abundance of genes related to hydrogen transfer and direct electron transfer increased in CFR, possibly enhancing electron transfer. These results contribute to a deeper understanding of how feeding regimes shape ethanol-type anaerobic ecosystems, providing valuable insights for optimizing anaerobic digestion processes to enhance methane production and electron transfer.

1. Introduction

Anaerobic digestion (AD) offers a dual advantage of decomposing organic matter while producing bioenergy. The AD process is composed of four stages: hydrolysis, acidogenesis, acetogenesis, and methanogenesis. The primary products of acidogenesis include ethanol and volatile fatty acids (VFAs), which are precursors for acetate production [1]. The metabolism of VFAs such as propionate and butyrate to acetate is thermodynamically infeasible, and their slow utilization can result in acid accumulation, further inhibiting methanogenesis [2,3]. In contrast, the transformation of ethanol to acetate is more thermodynamically favorable compared to propionate and butyrate, which makes ethanol-type fermentation an advantageous pathway in AD [1,4]. For instance, digesters fed with ethanol could improve organic degradation and methane production [2,4,5]. Anaerobic ethanol metabolism is mediated by diverse microbial consortia, leading to multiple products including acetate, propionate, and hydrogen. Moreover, the conversion of ethanol to methane relies on syntrophy between syntrophs and methanogens, with methanogens consuming hydrogen or acetate produced by syntrophs, facilitating ethanol oxidation [5]. Furthermore, ethanol is the optimal substrate for efficient chain elongation, which can react with VFAs to produce medium-chain fatty acids via reverse β-oxidation, offering a potential approach for resource recovery [6]. Therefore, gaining insight into the potential metabolic pathways of ethanol is crucial for optimizing resource recovery, given its pivotal role in the AD process.

Interspecies electron transfer between syntrophs and methanogens for ethanol oxidation could be conducted via interspecies hydrogen transfer (IHT) or direct interspecies electron transfer (DIET) [7]. Hydrogen transfer has been considered the primary form of interspecies electron transfer. The consumption of H_2 by methanogens reduces the partial pressure of H_2 in the systems, making the acetogenic reaction thermodynamically feasible [8]. Strains of syntrophic hydrogen producers involved in IHT with methanogens have been identified,

* Corresponding author.
E-mail address: guangxue.wu@universityofgalway.ie (G. Wu).

https://doi.org/10.1016/j.jece.2025.116688
Received 21 March 2025; Received in revised form 14 April 2025; Accepted 16 April 2025
Available online 17 April 2025

including ethanol-oxidizing microorganisms such as *Desulfovibrio*, *Sporomsa*, and *Syntrophus* [9,10]. Ethanol metabolism via the DIET pathway possesses greater energy efficiency compared to IHT between syntrophs and methanogens, thereby enhancing the overall ethanol degradation. DIET can be facilitated by functional microbial components, including conductive pili (e-pili) and c-type cytochromes (cytochrome c) [9]. DIET was potentially present in co-cultures of *Geobacter* with *Methanosarcina* or *Methanothrix* [11,12]. However, recent studies have primarily focused on the promotion of DIET with ethanol as the substrate, while a comprehensive investigation into the influence of ethanol on both IHT and DIET remains largely unexplored.

Ethanol metabolic pathways and syntrophic interactions in AD are shaped by diverse microorganisms. Designing reactors to selectively enrich relevant microorganisms based on their growth kinetics can help regulate their interactions effectively [13]. Microbial acclimation can be regulated by different feeding regimes of sequencing batch reactors (SBRs) and continuous-flow reactors (CFRs). In SBRs, substrate concentration gradually fluctuates during reaction, whereas in CFRs, a stable, low substrate concentration is maintained [13]. A previous study has observed that in SBR configurations, ethanol could be metabolized through both propionate and acetate production pathways, whereas in CFRs, the conversion of ethanol to propionate was absent [14]. Feeding regimes not only alter the metabolic pathways of ethanol but also manipulate microbial population. For instance, regarding the enriched microorganisms for ethanol oxidation, *Geobacter* was primarily enriched in CFRs, whereas *Desulfobulbus* and *Syntrophobacter* were predominantly enriched in SBRs [14]. In addition, the simultaneous co-enrichment of *Geobacter* and *Methanothrix* in CFRs might enhance the DIET process [11,15]. Furthermore, in SBRs, the initial exposure to high substrate concentrations typically enriched fast-growing methanogens, such as *Methanobacterium* [14,16,17]. Therefore, the mechanisms of feeding regimes regulating ethanol degradation pathways, microbial communities, and interspecies electron transfer deserve to be thoroughly elucidated in AD systems.

To bridge the above knowledge gaps, this study aimed to investigate the influence of feeding regimes on ethanol metabolism. A comprehensive analysis was conducted, including systems performance, microbial community structure, ethanol metabolic pathways, and syntrophic microbial metabolism in the systems. The findings contribute to a deeper understanding of ethanol metabolism and offer guidance for formulating strategies to manipulate ethanol degradation in anaerobic digestion systems.

2. Materials and methods

2.1. Reactor setup and operation

The long-term experiment was conducted with two stirred anaerobic reactors (one SBR and one CFR), with an effective working volume of 5 L each. The inoculum sludge was collected from laboratory-scale anaerobic reactors, and the inoculated volatile suspended solids (VSS) concentration was 3.1 ± 0.2 g/L. The temperature of 35°C was maintained by placing the reactors in a water bath. Both reactors were operated with a hydraulic retention time of 48 h and a 24 h reaction cycle, with a 50 % exchange ratio of treated wastewater per reaction cycle. In the SBR system, each cycle comprised of 23 h mixing with an initial 10 min feeding. The CFR system was operated with simultaneous mixing and feeding for 23 h. Both reactors shared identical settling of 50 min and discharge of 10 min. The experimental schematic diagram is shown in Fig. S1. During the operation, no sludge was discharged from both reactors except those washed out from the effluent.

Ethanol was used as the sole organic carbon in synthetic wastewater, with a concentration of 5000 mg COD/L. The inorganic components in the synthetic wastewater were 115 mg/L Na_2HPO_4, 478 mg/L NH_4Cl, 1500 mg/L $KHCO_3$, 1500 mg/L $NaHCO_3$, 197 mg/L $CaCl_2{\cdot}6\ H_2O$, 250 mg/L $MgSO_4$, and 1 mL/L trace element solution. The trace element solution contained the following components: 100 mg/L $MnCl_2{\cdot}4\ H_2O$, 100 mg/L $CoCl_2{\cdot}6\ H_2O$, 100 mg/L Na_2SeO_3, 100 mg/L $Na_2MoO_4{\cdot}2\ H_2O$, 100 mg/L H_3BO_3, 100 mg/L $Na_2WO_4{\cdot}2\ H_2O$, 200 mg/L $NiCl_2{\cdot}6\ H_2O$, and 1 g/L $FeCl_2{\cdot}4\ H_2O$ [14].

2.2. Batch experiments

Batch experiments were performed to evaluate microbial activities and metabolic pathways (Table S1). Firstly, reaction-cycle experiments were conducted to simulate the 24-h operational cycle of the parent reactors to assess ethanol degradation activities and methane production. Secondly, the specific acetoclastic methanogenic activity (SAMA) and hydrogenotrophic methanogenic activity (SHMA) were evaluated using acetate and H_2/CO_2 ($v/v = 80/20$, with a partial pressure of 1000 hPa) as the substrate, respectively. In these experiments, the sludge was washed three times to eliminate organic carbon, and then resuspended in the synthetic wastewater with only inorganic components to a final concentration of 2 g VSS/L.

For all batch experiments, 160 mL serum bottles were used, with a working volume of 100 mL and a headspace of 60 mL. The sludge was transferred into these bottles and purged with nitrogen gas for 3 min to maintain anaerobic conditions. The bottles were sealed with rubber stoppers and incubated in a shaker at 35°C and 170 rpm/min. Samples of the headspace gas and liquid water were periodically collected to measure gaseous methane content and liquid ethanol and VFAs concentrations. All batch experiments were conducted in duplicate. Methane production was monitored by measuring the headspace pressure and methane content, following the method described by Wang et al. [18].

2.3. Analytical methods

Suspended solids (SS) and VSS concentrations were determined following standard methods [19]. Methane content was analyzed using a gas chromatograph with a thermal conductivity detector (7890 A, Agilent, USA). Ethanol was analyzed using a Gallery Plus analyzer (Thermo Fisher Scientific, USA). VFAs concentrations were quantified using a high-performance liquid chromatography (HPLC, Agilent 1260, USA) with a UV detector. Separation was performed on a Aminex HPX-87H column (300 × 7.8 mm, Agilent) at 55°C, with 1 ‰ H_2SO_4 as the mobile phase at a flow rate of 0.8 mL/min. The injection volume was 30 μL, and the detection was carried out at 210 nm. Inorganic carbon was analyzed using a Shimadzu TOC-L analyzer equipped with an ASI-L autosampler (Shimadzu, Japan). The methane production from batch experiments was assessed using the modified Gompertz model [20],

$$P = P_{max}\exp[-\exp(\frac{eR_{max}(\lambda - t)}{P_{max}} + 1)] \quad (1)$$

where P represents cumulative methane production (mL/L), P_{max} is the maximum methane production potential (mL/L), R_{max} is the maximum methane production rate (mL/(L·h)), λ indicates the lag phase (h), t is the reaction time (h), and e is the natural logarithm. The kinetic parameters of methane production were determined using the OriginPro 2021 software.

2.4. Metagenomic analysis

Total DNA was extracted from sludge collected from both reactors under steady state conditions (day 74) using the DNeasy PowerSoil Pro Kit (QIAGEN, United Kingdom). The concentration and purity of the DNA were evaluated using the NanoDropOne spectrophotometer (Thermo Fisher Scientific, USA). Library was constructed using NEB Next® Ultra™ DNA Library Prep Kit and subject to sequencing on an Illumina Hiseq 2500 platform (Illumina, USA). Sequencing reads were trimmed with Trimmomatic (https://github.com/usadellab/Trimmomatic/). Clean reads were subject to assembly with MEGAHIT (https://github.com/voutcn/megahit) and the resulting effective scaftigs (≥500 bp) were used to identify open reading frames (ORFs) with Prodigal (https://github.com/hyattpd/Prodigal). Gene clustering and redundancy elimination were performed using MMseqs (https://github.com/soedinglab/MMseqs2) to generate non-redundant Unigenes. Unigenes were subsequently annotated against the NCBI-NR (https://www.ncbi.nlm.nih.gov/) and KEGG (https://www.kegg.jp/) databases to acquire the microbial community composition and functional gene categories (e-value cutoff of 10^{-5}) [21,22]. The raw sequencing data were deposited to NCBI with the accession number of PRJNA1248186.

3. Results and discussion

3.1. Long-term operation of SBR and CFR

The two reactors were operated continuously for 77 days. System performance of the two reactors is presented in Table 1. The COD removal percentage of CFR was 100 %, demonstrating the strong capacity of microorganisms for organic carbon degradation in CFR. In comparison, SBR could remove only 36.8 ± 0.1 % of COD in the feed. Ethanol was completely removed in CFR, and no VFAs were detected in the effluent (Fig. S2). In contrast, effluent ethanol fluctuated in SBR, with an average concentration of 540.7 mg COD/L (Fig. S2b). High concentrations of acetate (2473.0 ± 427.7 mg COD/L) were detected in the effluent of SBR during day 1 to day 63. From day 64 to day 77, an accumulation of 2250.1 ± 129.9 mg COD/L acetate and 931.3 ± 183.8 mg COD/L butyrate was observed in SBR (Fig. S2c). The effluent pH of SBR was 5.1 ± 0.1, markedly lower than that of CFR, which was 7.4 ± 0.1, despite both reactors having the same influent pH of 8.3 ± 0.1. The VSS concentrations under steady state conditions were 3.0 ± 0.2 g/L in CFR, higher than 1.4 ± 0.3 g/L in SBR. The lower VSS concentration in SBR was primarily due to the inhibitory effects of low pH and VFA accumulation on microbial activity. Overall, CFR outcompeted SBR in COD removal during the long-term operation.

Methane production was 2.5-folds higher in CFR than in SBR during the long-term operation. The accumulation of acid in SBR reduced the pH, leading to reduced methanogenic activities and methane production. The inorganic carbon in the reactors was examined during a typical cycle. At the end of one cycle reaction, inorganic carbon was 263.3 mg/L in CFR, while it was only 7.9 mg/L in SBR. This indicated that the buffer HCO_3^- in the feed water was extensively consumed in SBR, which might explain the remarkable pH decrease observed in SBR. In conclusion, SBR exhibited lower methane production than CFR, potentially due to the low pH condition in SBR.

Notably, the presence of ethanol and acetate and the low pH in SBR facilitated ethanol metabolism towards butyrate production. It has been reported that butyrate production from ethanol was optimal at the pH of 6 [23]. The catabolic reactions in anaerobic ethanol oxidation are listed in Table S2. The metabolism involves the oxidation of ethanol to butyrate via coupled reactions. Firstly, ethanol is converted to acetyl-CoA, which is then elongated in a cyclic pathway to form butyrate [24].

Table 1
Summary of COD, pH, COD removal percentages, SS, and VSS during the long-term operation of SBR and CFR.

		SBR	CFR
Influent	COD (mg/L)	4985.6 ± 144.4	
	pH	8.3 ± 0.05	
Effluent	COD (mg/L)	3129.4 ± 338.0	Not detected
	COD removal percentage (%)	36.8 ± 0.08	100
	pH	5.1 ± 0.1	7.4 ± 0.1
Sludge	Initial SS (g/L)	5.3 ± 0.02	
	Initial VSS (g/L)	3.1 ± 0.2	
	Steady state SS (g/L)	1.8 ± 0.6	3.6 ± 0.4
	Steady state VSS (g/L)	1.4 ± 0.3	3.0 ± 0.2

Under anaerobic conditions, the reaction between acetate and ethanol can produce H_2, butyric acid, caproic acids, etc. The type of produced substance depends on the available amounts of acetate and ethanol. If an excess of acetate is present, a high amount of butyric acid can be formed, whereas if ethanol is in excess, the main product is caproic acid [25]. Differing from CFR, which favored methanogenesis, the high acetate concentration in SBR led to low pH, inhibiting methanogenesis but triggering carbon chain elongation.

3.2. Microbial activity analysis

3.2.1. Assessment of microbial activity through cycle experiments

To evaluate microbial activities of SBR and CFR, the typical reaction cycle experiment was performed. Figs. 1a and 1b show dynamics of ethanol, VFAs, and methane within a typical reaction cycle. When the cycle was finished, the COD removal percentages in SBR and CFR were 26.5 % and 100 %, respectively. The ethanol degradation rate of SBR and CFR was 92.4 and 354.9 mg COD/(L·h), respectively. In CFR, ethanol could be completely degraded within 7 h, with acetate as the sole VFA produced. Therefore, ethanol-to-acetate pathway predominantly governed ethanol oxidation in CFR. While in SBR, at the end of the cycle, the ethanol concentration was 604.3 mg COD/L. The peak acetate concentration in SBR and CFR was 2889.1 ± 248.8 and 1109.1 ± 4.1 mg COD/L at 20 h and 7 h, respectively. At 20 h, acetate was completely degraded in CFR. Minor fluctuation in butyrate concentration (averaging 262.9 ± 11.2 mg COD/L) was observed during the cycle reaction in SBR, deviating from the results of butyrate concentration in the parent reactor (Fig. S3). This divergent phenomenon requires further investigation. In a previous study [14], the production of propionate and acetate in rapid-filling ethanol-fed reactors was observed, while acetate generation was mainly observed in continuous-filling reactors. The difference might be attributed to the higher bicarbonate concentration in the study of Du et al. [14], as their findings indicated that bicarbonate facilitated the ethanol-to-propionate pathway and was essential for propionate production in SBRs.

For methanogenesis, the volume-based maximum methane production rate was 29.0 ± 2.6 mL/(L·h) in SBR and 56.7 ± 6.8 mL/(L·h) in CFR (Table S3). In addition, the lag phase of CH_4 production in CFR (0.8 ± 0.8 h) was noticeably lower than in SBR (5.5 ± 0.3 h). In SBR, the CH_4 production was halted at 12 h, indicating that methanogenic activity was inhibited as the pH decreased to an unsuitable level for methanogens. The results were consistent with the long-term operation and indicated that the CFR configuration facilitated ethanol degradation and methane production. This improvement may be attributed to the continuous lower substrate concentration maintained in CFR, contributing to a greater stable environment compared to SBR, aligning with the finding of Li et al. [26] that the continuous-feeding mode enhanced system stability.

3.2.2. Methanogenesis activities

To examine the methanogenic activities of SBR and CFR, batch experiments were conducted. Figs. 1c and 1d depict acetoclastic methanogenesis and hydrogenotrophic methanogenesis activities, respectively. For SAMA, the maximum CH_4 production rate was 21.4 ± 0.3 mL/(L·h) in CFR. While, the acetoclastic methanogenesis activity was exclusively absent in SBR, probably due to that the low pH hindered the activity of the pH-sensitive acetoclastic methanogens [27]. Regarding SHMA, the maximum CH_4 production rate was 14.3 ± 3.5 mL/(L·h) in SBR and 34.2 ± 2.5 mL/(L·h) in CFR, and the lag phase was 6.6 ± 0.8 h in SBR and 4.1 ± 0.2 h in CFR. The results illustrated that CFR exhibited superior SHMA than SBR, along with a shorter lag phase, which could be due to the acclimation of higher relative abundance of hydrogenotrophic methanogens in CFR.

Based on the above results, feeding regimes effectively modulated ethanol oxidation and methanogenesis pathways. In SBR, ethanol was oxidized to acetate and butyrate, with methane production occurring

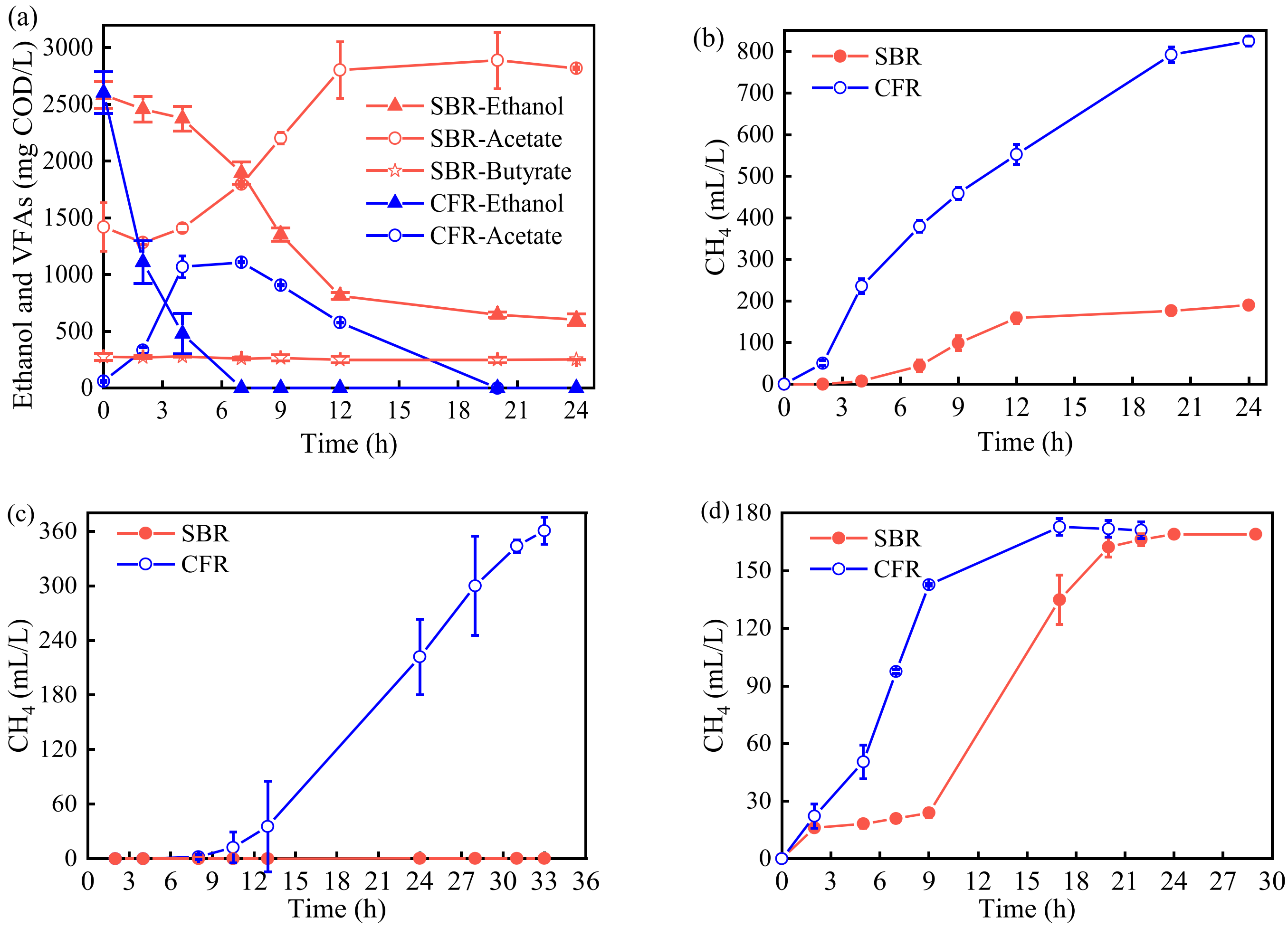

Fig. 1. Dynamics of ethanol and VFAs (a) and CH_4 (b) within a typical cycle of SBR and CFR, as well as CH_4 production fed with acetate (c) and H_2/CO_2 (d).

exclusively via the hydrogenotrophic methanogenesis pathway, while acetoclastic methanogenesis was inhibited. In contrast, in CFR, ethanol was metabolized solely to acetate, and methane was produced through both acetoclastic and hydrogenotrophic methanogenesis pathways.

3.3. Microbial community structure

The microbial community of SBR and CFR was analyzed based on metagenomic sequencing. Table S4 summarizes sequencing results and α diversity indices of the two reactors. The total sequencing number of contigs in SBR and CFR was 374305 and 306854, respectively.

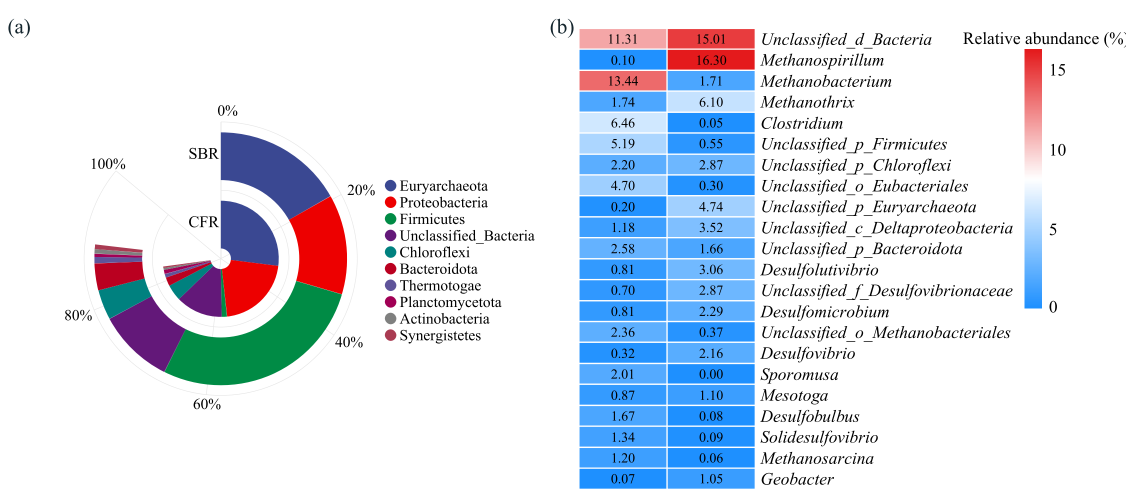

Fig. 2. Relative abundances of the 10 most abundant taxa at phylum level (a) and 22 most abundant taxa at genus level (b) based on metagenomic sequence data in two reactors. The numbers in the heatmap represent the relative abundances of each taxon.

Compared to SBR, CFR showed higher values of observed species, ACE, and Chao1 indices, indicating a greater microbial diversity. The low pH of SBR might hinder the growth of certain types of microbes.

At the phylum level (Fig. 2a), Firmicutes, Euryarchaeota, and Proteobacteria were the dominant phyla in SBR, accounting for 32.3 %, 19.5 %, and 14.8 %, respectively. In CFR, Euryarchaeota (31.3 %) was the predominant phylum, followed by Proteobacteria (24.7 %) and Chloroflexi (5.3 %). The relative abundance of Firmicutes in SBR (32.3 %) was much higher than in CFR (1.7 %). *Clostridium*, a member of Firmicutes, is known for its potential to produce butyrate as a by-product through fermentation, which might explain butyrate production observed in SBR [28,29]. Euryarchaeota, which includes methanogens, was more abundantly enriched in CFR compared to SBR.

At the genus level (Fig. 2b), methanogens accounted for a higher total relative abundance in CFR (24.9 %) compared to SBR (16.6 %), aligning with the enhanced methane production observed in CFR during the long-term operation. *Methanobacterium*, a representative H_2-scavenger methanogen, dominated in SBR (13.4 %), whereas *Methanospirillum* was more prevalent in CFR (16.3 %). *Methanobacterium*, a fast-growing methanogen with strong adaptability, exhibited tolerance to acidic environments (pH of 5.6 ~ 6.2) [30–32]. In the study of Xing et al. [16], *Methanobacterium* emerged as the predominant methanogen in response to acetate accumulation and low pH in the system, demonstrating its adaptability to adverse environmental conditions. On the other hand, slow-growing *Methanospirillum* demonstrated a higher affinity for H_2 and a lower hydrogen consumption efficiency compared to *Methanobacterium* [31]. Furthermore, *Methanospirillum* was identified as the predominant methanogen in the CFR system with a 10-day sludge retention time [15]. These hydrogenotrophic methanogens could obtain H_2 from syntrophic interspecies hydrogen transfer, maintaining a low hydrogen partial pressure, thereby driving energetically favorable ethanol oxidation [9]. *Methanothrix* and *Methanosarcina*, two acetoclastic methanogens, exhibited distinct distribution patterns. *Methanothrix* displayed a higher relative abundance in CFR (6.1 %) compared to SBR (1.7 %), whereas *Methanosarcina* was more prevalent in SBR (1.2 %) than in CFR (0.06 %). The genomes of *Methanosarcina* and *Methanothrix* were detectable in SBR, but the acetate-to-CH_4 pathway was not observed. It was potentially due to the environmental stresses of low pH and acid accumulation, resulting in a dormant or inactive state for these microorganisms. The enrichment of hydrogenotrophic methanogens over acetoclastic methanogens may primarily be attributed to the shorter double time of hydrogenotrophic methanogens [17].

Clostridium, *Sporomusa*, *Desulfobulbus*, and *Solidesulfovibrio* were the dominant genus in SBR. According to previous studies, *Clostridium* species are particularly prominent butyrate producers [33,34]. Some *Clostridium* could also enhance methane yield through syntrophic acetate oxidation by providing hydrogen-consuming methanogens with H_2 and CO_2 [35]. *Clostridium* species generally thrive in acidic environment, with their optimal growth typically occurring at the pH of 6 [23,36]. *Sporomusa* can collaborate with hydrogenotrophic methanogens through potential interspecies H_2 transfer [37]. *Desulfobulbus* can incompletely oxidize numerous organics including glucose, ethanol, and propionate to acetate [38]. Moreover, *Sporomusa* and *Desulfobulbus* are reported to be capable of surviving under low pH conditions [39]. In CFR, *Desulfolutivibrio*, *Desulfomicrobium*, *Desulfovibrio*, and *Mesotoga* were the predominant genera, and they can oxidize ethanol into acetate, potentially functioning as syntrophic partners with methanogens [40,41]. *Desulfomicrobium* and *Mesotoga* were also found to have a competitive advantage in CFR [40,42], potentially due to that the continuous feeding strategy promotes their growth. Additionally, the electroactive ethanol oxidizer *Geobacter* could be enriched in CFR, which could facilitate DIET with *Methanosarcina* or *Methanothrix* [11,37]. Overall, the distinct microbial compositions in SBR and CFR highlighted the varying metabolic interactions and electron transfer mechanisms, with SBR favoring butyrate production, while CFR promoting efficient ethanol oxidation and potential DIET-driven methanogenesis.

Sulfate-reducing bacteria (SRB) were present in both SBR and CFR. The relationships between SRB and archaea are found to be more complex, either cooperative or competitive interactions with hydrogenotrophic and acetoclastic methanogens [43]. Certain SRB, such as *Desulfovibrio*, are capable of oxidizing ethanol to H_2 and CO_2, establishing a syntrophic relationship with hydrogenotrophic methanogens in the absence of sulfate [44]. Meanwhile, some SRBs, like *Desulfomicrobium*, can convert ethanol to acetate, facilitating the potential syntrophic association with acetoclastic methanogens [45]. However, the relationships between SRB and archaea were found to be more complex than mere cooperative [45]. The CFR exhibited a conducive environment to the growth of various microorganisms, resulting in greater bacterial diversity and high abundance of redundant communities. This also indicated that syntrophic interactions may not be the sole dominant metabolic process in CFR, as various bacteria could be enriched through alternative metabolic pathways [16].

3.4. Genes abundances analysis

3.4.1. Genes associated with ethanol metabolic pathways

To further investigate the metabolic pathways, genes encoding key functional enzymes of the carbon metabolism were analyzed. The enzyme names corresponding to the EC number referenced from the KEGG database are summarized in Table S5. The enzymes involved in ethanol oxidation to acetate are shown in Fig. 3a. Ethanol is oxidized to acetaldehyde by ethanol dehydrogenase (EC: 1.1.1.1). Following, there are two pathways for acetaldehyde conversion: to acetyl-CoA by acetaldehyde dehydrogenase (EC: 1.2.1.10), or to acetate by aldehyde dehydrogenase (EC: 1.2.1.3) or by aldehyde ferredoxin oxidoreductase (EC: 1.2.7.5). Higher relative abundances of EC: 1.1.1.1 and EC: 1.2.1.10 were found in SBR (0.019 % and 0.007 %) compared to CFR (0.005 % and 0.0008 %). In the conversion of acetyl-CoA to acetate, acylphosphatase (EC: 3.6.1.7) and acetyl-CoA synthetase (EC: 6.2.1.1) were involved, and was 5.4 times and 1.7 times greater in CFR than in SBR, respectively. The results suggested that different metabolic pathways were displayed in the conversion of ethanol to acetate in SBR and CFR, which was in agreement with the previous study [15]. In SBR, *Clostridium* harbored key genes involved in ethanol metabolism, highlighting its important role in the system [6]. Moreover, the enzymes related to ethanol oxidation were mainly assigned to *Desulfolutivibrio* in CFR (Fig. S4a and S4b), aligning with the observed microbial community structure. EC: 1.2.1.10 was mainly detected in *Desulfovibrio*, which was consistent with the study of Du et al. [46]. Additionally, relevant genes harbored by *Desulfobulbus* were higher in SBR compared to CFR, which was consistent with a previous study [14].

3.4.2. Genes associated with acetate metabolism pathways

Acetate degradation is conducted by acetoclastic methanogenesis or by syntrophic oxidation through activities of acetate oxidizers coupled with hydrogenotrophic methanogens in anaerobic digestion systems. There are two potential pathways reported for acetate oxidation to hydrogen and carbon dioxide: the reversed Wood-Ljungdahl pathway (WLP) and the reversed WLP with the glycine cleavage system (WLP-GCS) (Fig. 3b) [43]. Acetate is transformed into acetyl-CoA through the action of acetyl-CoA synthetase (EC: 6.2.1.1) or via acetate kinase (EC: 2.7.2.1) in combination with phosphate acetyltransferase (EC: 2.3.1.8). Subsequently, acetyl-CoA is further converted into 5-Methyl-tetrahydromethanopterin or pyruvate by acetyl-CoA decarbonylase/synthase (EC: 2.3.1.169/2.1.1.245) or pyruvate ferredoxin oxidoreductase (EC: 1.2.7.1). These enzymes (EC: 2.3.1.169, 2.1.1.245, and 1.2.7.1) exhibited appreciably higher abundances in CFR (0.007 %, 0.006 %, and 0.091 %, respectively) compared to SBR (0.003 %, 0.003 %, and 0.037 %, respectively). The genes encoding glycine reductase (EC: 1.21.4.2), involved in the conversion of acetyl phosphate to glycine, exhibited a higher relative abundance in SBR (0.018 %) compared to CFR (0.008 %).

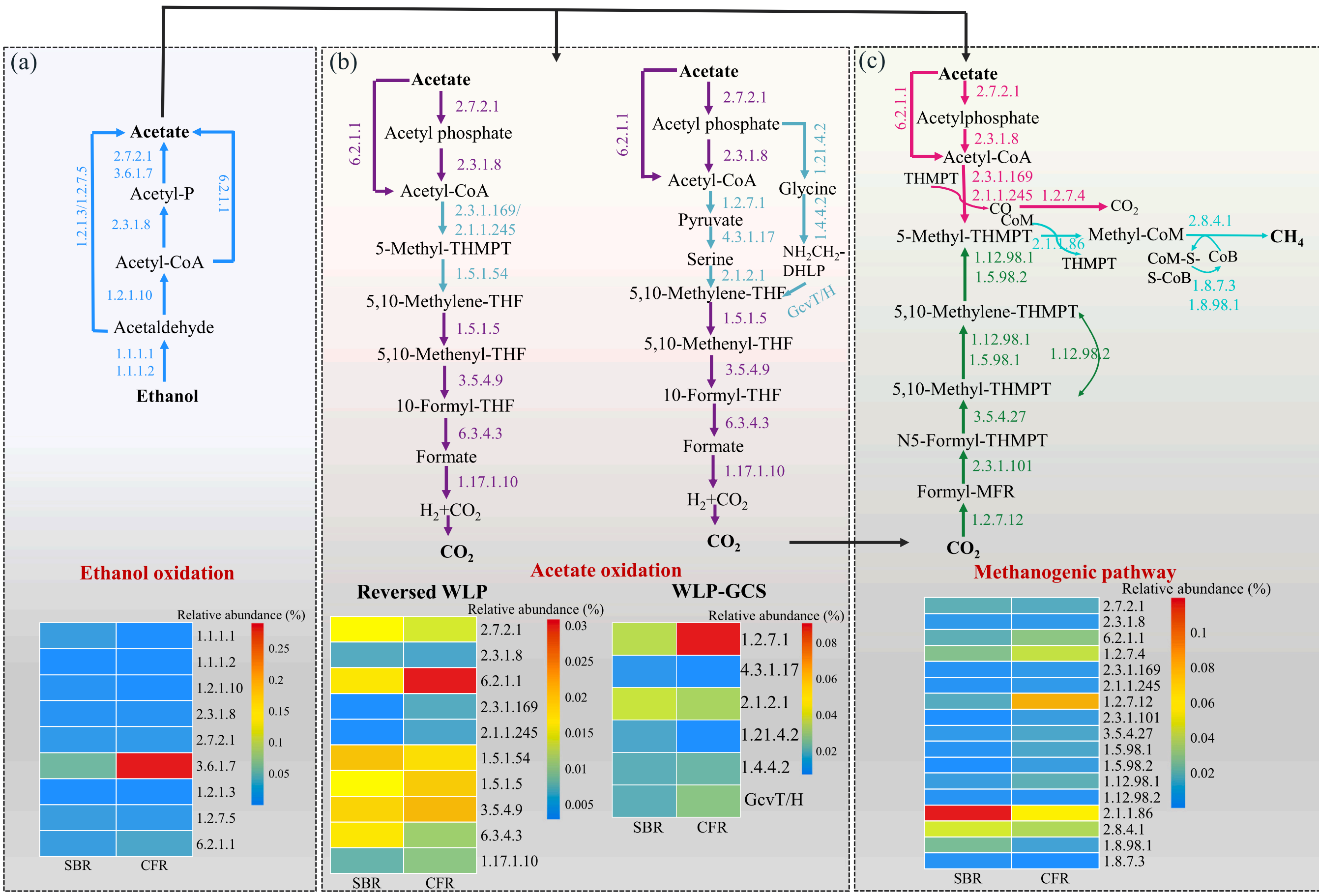

Fig. 3. Metabolic pathway and the related functional genes of ethanol oxidation (a), syntrophic acetate oxidation via the reversed Wood-Ljungdahl pathway (WLP) and the reversed WLP with a glycine cleavage system (WLP-GCS) (b), the text of enzymes in purple represents enzymes in the common pathway, while indigo blue indicates enzymes unique to the two pathways, as well as methane production (c), the text of enzymes in pink represents enzymes in acetoclastic pathway, green denotes enzymes in hydrogenotrophic pathway, and bright blue indicates enzymes in the common pathway.

The results demonstrated a clear variation in acetate oxidation of bacteria between CFR and SBR. Compared to SBR, the genes associated with acetate oxidation exhibited an increased abundance in CFR. This evidence further implied that CFR might facilitate syntrophic relationships between potential syntrophic acetate-oxidizing bacteria and methanogens, thus promoting efficient methanogenesis. Specifically, the genes involved in WLP-GCS demonstrated greater abundance than the reversed WLP, emphasizing the essential role of the glycine cleavage pathway in acetate oxidation. The glycine cleavage pathway generates one ATP per acetate, while WLP does not produce ATP with acetate oxidization [41]. This efficient energy generation strategy might partially account for the high genes abundance of the glycine cleavage pathway [43]. The predicted metabolic pathways further suggested that enzymes participating in acetate oxidation were mainly assigned to *Clostridium*, *Desulfomicrobium*, and *Desulfolutivibrio* in SBR, and *Desulfolutivibrio*, *Desulfomicrobium*, and *Geobacter* in CFR (Fig. S4c, d, e and f). They might potentially produce H_2 and act as a syntrophic partner to hydrogenotrophic methanogens.

3.4.3. Genes associated with methanogenic pathways

Fig. 3c shows the relative abundances of genes related to acetoclastic and hydrogenotrophic methanogenesis. A remarkable relative abundance of formylmethanofuran dehydrogenase (EC: 1.2.7.12) was detected in CFR. Moreover, superior relative abundances of enzymes (except for EC: 1.12.98.2) involving in the CO_2 reduction pathway were found in CFR compared to SBR. Common steps of acetoclastic and hydrogenotrophic methanogenesis pathways, including tetrahydromethanopterin S-methyltransferase (EC: 2.1.1.86), coenzyme-B sulfoethylthiotransferase (EC: 2.8.4.1), and CoB-CoM heterodisulfide reductase (EC: 1.8.98.1 and 1.8.7.3) were observed with higher relative abundances in SBR than in CFR, which were mainly assigned to *Methanobacterium*. Xing et al. [16] suggested an efficient energy contribution of *Methanobacterium* under stressed conditions, inducing high methanogenic activity. Regarding acetate metabolism, the genes encoding EC: 6.2.1.1, EC: 2.7.2.1, and EC: 2.3.1.8 were detected with low abundances in methanogens in SBR and CFR (Fig. S4g and S4h), aligning with the observed low abundance of acetoclastic methanogens. The genes in methanogenic pathways were mainly assigned to *Methanobacterium* in SBR and *Methanospirillum* in CFR, aligning with their dominance in each reactor. *Methanothrix*, the specialist acetoclastic methanogens, was also found to possess genes for CO_2 reduction, implying its potential metabolism via DIET [11,37]. It is important to note that the results were based on metagenomic analysis, which may have limitations, and further comprehensive studies from metatranscriptome level should be carried out to elucidate the metabolic pathway.

3.4.4. Genes associated with butyrate production pathway in SBR

Butyrate is produced through chain elongation via the reverse β-oxidation pathway with ethanol serving as the external electron donor [47] (Fig. 4a). In the first step of the reverse β-oxidation pathway, 6 molecules ethanol are oxidized to 5 molecules acetyl-CoA and 1 molecule acetate, and then acetyl-CoA enters the chain elongation cycle and serves as a two-carbon donor for butyrate synthesis [48]. The following

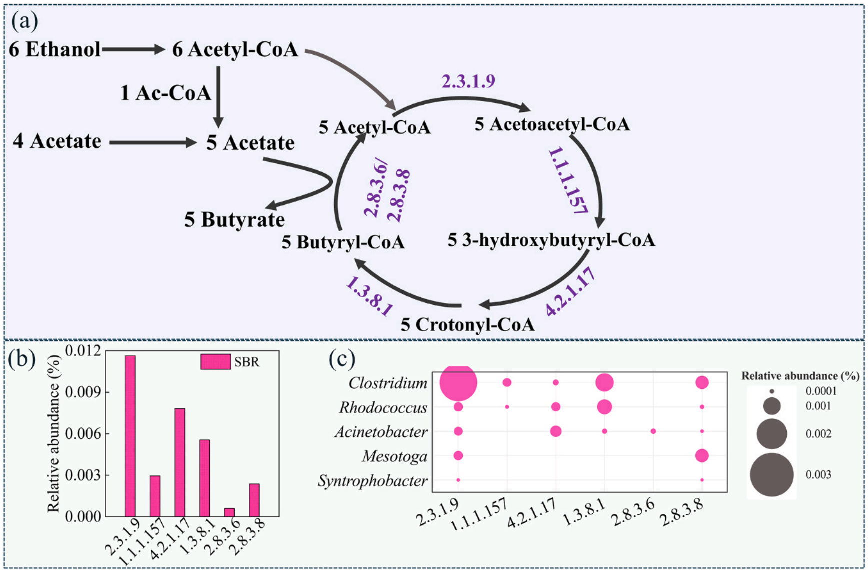

Fig. 4. Metabolic pathway of butyrate production via the reverse β-oxidation pathway (a), the numbers before the chemicals represent their stoichiometric coefficients, indicating the relative molecular quantities involved in the pathway, and the relative abundances of the functional genes (b), and the genes assigned to the functional bacteria (c).

intermediates are involved: acetoacetyl-CoA, 3-hydroxybutyryl-CoA, crotonyl-CoA, and butyryl-CoA. The enzymes participating in the process include acetoacetyl-CoA thiolase (Thl, EC: 2.3.1.9), 3-hydroxybutyryl-CoA dehydrogenase (Hbd, EC: 1.1.1.157), enoyl-CoA hydratase (Crt, EC: 4.2.1.17), butyryl-CoA dehydrogenase (Bcd, EC: 1.3.8.1), and acetate-CoA transferase (Cat, EC: 2.8.3.6/2.8.3.8), and their relative abundances in SBR were 0.011 %, 0.003 %, 0.008 %, 0.006 %, and 0.003 %, respectively (Fig. 4b). In addition, most butyrate-production related genes were assigned to *Clostridium* (Fig. 4c), the key microbes responsible for chain elongation for butyrate production [33].

With methanogenesis inhibited, methane (the most reduced product) cannot be formed, so the next preferable product, a longer carboxylate, is produced by the reverse β-oxidation chain elongation pathway to gain more ATP [49]. The chain elongation process is strongly affected by factors such as pH, partial pressure of hydrogen, ethanol-to-acetate ratio, and methanogenesis [50]. The production of butyrate in SBR is noteworthy and valuable for carbon chain elongation, deserving further studies.

3.4.5. Genes associated with interspecies electron transfer

Ethanol in AD can facilitate syntrophic interactions between syntrophic partners and methanogens. To gain deeper insight into the syntrophic metabolism pathways bridging these microorganisms, the present study examined the hydrogenase genes engaged in H_2 production and utilization, as well as the genes associated with DIET.

In bacteria, enzymes involved in H_2 generation include cytoplasmic

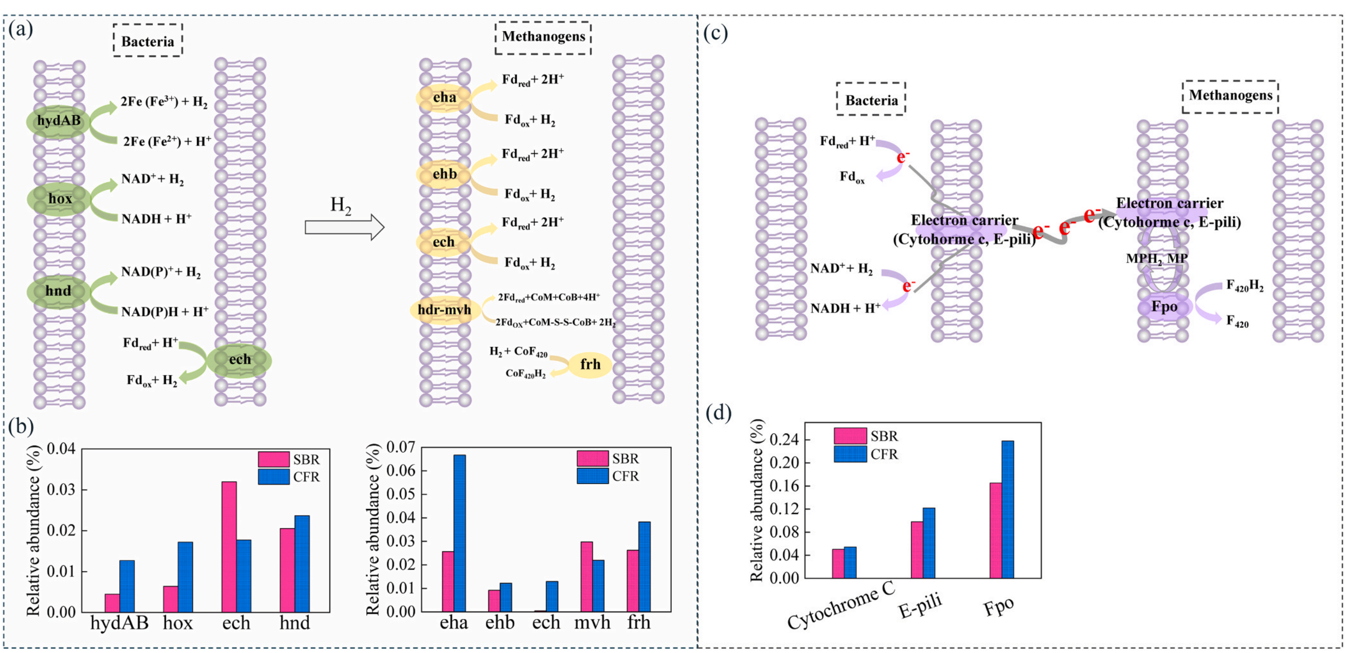

Fig. 5. The metabolism of H_2 (a) and the relative abundances of the related genes (b), as well as the pathway associated with direct electron transfer (c) and the relative abundances of the related genes (d).

[FeFe]-type electron-confurcating hydrogenases (hydAB), cytosolic NiFe hydrogenase (hox), energy-converting [NiFe] hydrogenase (ech), and NADPH-dependent [FeFe] hydrogenase (hnd) (Fig. 5a) [4,43]. The relative abundances of hydAB and hox genes in CFR were 2.8 and 2.7 times higher than in SBR, respectively (Fig. 5b). In methanogens, the primary hydrogenase genes participated in H_2 utilization are energy-converting hydrogenase (eha and ehb), ech, F_{420}-non-reducing hydrogenase (mvh), and coenzyme F_{420} hydrogenase (frh) (Fig. 5a), with eha, ehb, and ech performing critical roles in H_2 capture [51]. The relative abundances of genes encoding eha, ehb, and ech were 2.6, 1.3, and 39.4 folds higher in CFR than in SBR, respectively (Fig. 5b), suggesting an elevated capacity of methanogens to capture H_2 in CFR. The co-enrichment of H_2-production bacteria and *Methanospirillum*, along with the increased hydrogenase genes in CFR, indicated an augmented IHT pathway in CFR. The syntrophic interactions through IHT are considered a potentially more efficient strategy for energy production compared to mixotrophic pathways [16].

Fig. 5c illustrates the genes related to DIET in the two reactors. The genes encoding e-pili and cytochromes c are essential components facilitating electron transfer between syntrophic microorganisms [52, 53]. The abundance of the e-pili genes in CFR was 1.2 times greater than that in SBR (Fig. 5d). However, genes responsible for cytochromes c synthesis were not upregulated in CFR. Zhao et al. [5] and Zhang et al. [4] also reported that the abundance of e-pili was higher in ethanol-type reactors than in other reactors, while the genes assigned to cytochromes c remained unregulated. Thus, CFR system might primarily facilitate DIET via e-pili rather than cytochromes c. An increase in sludge conductivity further supported the enhancement of DIET in CFR (Fig. S5a). The electrical conductivity of CFR sludge (3.0 μg/(mL·min)) was 233 % higher than that of SBR sludge (0.9 μg/(mL·min)). Furthermore, the redox capability of the system was assessed by cyclic voltammetry (CV). The oxidation and reduction current peak values were higher in CFR than in SBR at the same scan rate (Fig. S5b and c). The elevated peak currents of CV also indicated enhanced electron transfer in CFR. Therefore, the CFR system had a more integrated interspecies electrical connection compared to SBR. Moreover, the co-existence of *Methanothrix* and *Geobacter* in CFR also suggested the potential DIET in the system [5,11].

4. Conclusion

This study provided an in-depth analysis of system performance, metabolic pathways, and syntrophic metabolism in ethanol-type AD under varying feeding regimes. The results showed that CFR exhibited advantages over SBR in terms of ethanol degradation and methanogenesis. Ethanol was converted not only to acetate but also to butyrate by *Clostridium* in SBR. *Methanobacterium* was primarily enriched in SBR and responsible for hydrogenotrophic methanogenesis. In contrast, CFR exhibited a higher relative abundance of *Desulfolutivibrio* and *Methanospirillum*, and the electroactive bacteria: *Geobacter*. The metagenomic analysis further revealed enhanced electron transfer processes (IHT and DIET) in CFR.

CRediT authorship contribution statement

Huanhuan Chang: Writing – original draft, Methodology, Investigation, Formal analysis. **Yuepeng Sun:** Writing – review & editing, Methodology. **Tingxia Liu:** Writing – review & editing, Formal analysis. **Guangxue Wu:** Writing – review & editing, Supervision, Methodology, Funding acquisition, Conceptualization.

Declaration of Competing Interest

The authors declare the following financial interests/personal relationships which may be considered as potential competing interests: Huanhuan Chang reports financial support was provided by China Scholarship Council. Guangxue Wu reports financial support was provided by Galway University Foundation CLG. Guangxue Wu reports financial support was provided by Science Foundation Ireland. Guangxue Wu reports financial support was provided by Sustainable Energy Authority of Ireland. If there are other authors, they declare that they have no known competing financial interests or personal relationships that could have appeared to influence the work reported in this paper.

Acknowledgements

This study was supported by the Taighde Éireann – Research Ireland (formerly Science Foundation Ireland) and the Sustainable Energy Authority of Ireland under the SFI Frontiers for the Future Awards Programme (22/FFP-A/10346). Huanhuan Chang thanks the scholarship from the China Scholarship Council (No 202208620052). Guangxue Wu thanks the support from the Galway University Foundation.

Appendix A. Supporting information

Supplementary data associated with this article can be found in the online version at doi:10.1016/j.jece.2025.116688.

Data Availability

Data will be made available on request.

References

[1] M.J. McInerney, C.G. Struchtemeyer, J. Sieber, H. Mouttaki, A.J.M. Stams, B. Schink, L. Rohlin, R.P. Gunsalus, Physiology, ecology, phylogeny, and genomics of microorganisms capable of syntrophic metabolism, Ann. N. Y. Acad. Sci. 1125 (2008) 58–72.
[2] X. Ma, M. Yu, N. Song, B. Xu, M. Gao, C. Wu, Q. Wang, Effect of ethanol pre-fermentation on organic load rate and stability of semi-continuous anaerobic digestion of food waste, Bioresour. Technol. 299 (2020) 122587.
[3] S. Zhang, P. Zhao, C. Wu, M. Gao, Q. Wang, X. Sun, Optimizing ethanol pre-fermentation of food waste to enhance batch anaerobic digestion: regulation of the acidification pathway, Fuel 368 (2024) 131664.
[4] S. Zhang, Y. Ren, P. Zhao, X. Wang, Q. Wang, X. Sun, Ethanol-type anaerobic digestion enhanced methanogenic performance by stimulating direct interspecies electron transfer and interspecies hydrogen transfer, Bioresour. Technol. 410 (2024) 131280.
[5] Z. Zhao, J. Wang, Y. Li, T. Zhu, Q. Yu, T. Wang, S. Liang, Y. Zhang, Why do DIETers like drinking: Metagenomic analysis for methane and energy metabolism during anaerobic digestion with ethanol, Water Res. 171 (2020) 115425.
[6] M. Roghair, T. Hoogstad, D.P.B.T.B. Strik, C.M. Plugge, P.H.A. Timmers, R. A. Weusthuis, M.E. Bruins, C.J.N. Buisman, Controlling ethanol use in chain elongation by CO_2 loading rate, Environ. Sci. Technol. 52 (2018) 1496–1505.
[7] P. Xu, H. Liu, C. Liu, G. Zhu, Syntrophic methane production from volatile fatty acids: Focus on interspecies electron transfer, Sci. Total Environ. 946 (2024) 174410.
[8] B.E.L. Morris, R. Henneberger, H. Huber, C. Moissl-Eichinger, Microbial syntrophy: interaction for the common good, FEMS Microbiol. Rev. 37 (2013) 384–406.
[9] Y. Zhang, C. Li, Z. Yuan, R. Wang, I. Angelidaki, G. Zhu, Syntrophy mechanism, microbial population, and process optimization for volatile fatty acids metabolism in anaerobic digestion, Chem. Eng. J. 452 (2023) 139137.
[10] A.J.M. Stams, C.M. Plugge, Electron transfer in syntrophic communities of anaerobic bacteria and archaea, Nat. Rev. Microbiol. 7 (2009) 568–577.
[11] A.-E. Rotaru, P.M. Shrestha, F. Liu, M. Shrestha, D. Shrestha, M. Embree, K. Zengler, C. Wardman, K.P. Nevin, D.R. Lovley, A new model for electron flow during anaerobic digestion: direct interspecies electron transfer to *Methanosaeta* for the reduction of carbon dioxide to methane, Energy Environ. Sci. 7 (2014) 408–415.
[12] A.-E. Rotaru, M. Shrestha Pravin, F. Liu, B. Markovaite, S. Chen, P.Nevin Kelly, R. Lovley Derek, Direct Interspecies Electron Transfer between *Geobacter metallireducens* and *Methanosarcina barkeri*, Appl. Environ. Microbiol. 80 (2014) 4599–4605.
[13] Q. Yin, Y. Sun, B. Li, Z. Feng, G. Wu, The r/K selection theory and its application in biological wastewater treatment processes, Sci. Total Environ. 824 (2022) 153836.
[14] B. Du, X. Zhan, P.N.L. Lens, Y. Zhang, G. Wu, Deciphering anaerobic ethanol metabolic pathways shaped by operational modes, Water Res. 249 (2024) 120896.
[15] Q. Guo, Q. Yin, J. Du, J. Zuo, G. Wu, New insights into the r/K selection theory achieved in methanogenic systems through continuous-flow and sequencing batch operational modes, Sci. Total Environ. 807 (2022) 150732.
[16] L. Xing, L. Li, Q. Yin, G. Wu, Solids retention times shift methanogenic ethanol oxidation: novel insights into metabolic pathways, microbial community dynamics, and energy metabolisms, ACS Sustain. Chem. Eng. 9 (2021) 15861–15874.

[17] R.K. Thauer, A.-K. Kaster, H. Seedorf, W. Buckel, R. Hedderich, Methanogenic archaea: ecologically relevant differences in energy conservation, Nat. Rev. Microbiol 6 (2008) 579–591.
[18] Z. Wang, S. Wang, Y. Hu, B. Du, J. Meng, G. Wu, H. Liu, X. Zhan, Distinguishing responses of acetoclastic and hydrogenotrophic methanogens to ammonia stress in mesophilic mixed cultures, Water Res. 224 (2022) 119029.
[19] APHA, Standard Methods for the Examination of Water and Wastewater, American Public Health Association, Washington DC, 2005.
[20] M.H. Zwietering, I. Jongenburger, F.M. Rombouts, K. Van't Riet, Modeling of the bacterial growth curve, Appl. Environ. Microbiol 56 (1990) 1875–1881.
[21] M. Kanehisa, S. Goto, KEGG: Kyoto encyclopedia of genes and genomes, Nucleic Acids Res 28 (2000) 27–30.
[22] N.K. Kim, S.H. Lee, Y. Kim, H.D. Park, Current understanding and perspectives in anaerobic digestion based on genome-resolved metagenomic approaches, Bioresour. Technol. 344 (2022) 126350.
[23] K.J.J. Steinbusch, E. Arvaniti, H.V.M. Hamelers, C.J.N. Buisman, Selective inhibition of methanogenesis to enhance ethanol and n-butyrate production through acetate reduction in mixed culture fermentation, Bioresour. Technol. 100 (2009) 3261–3267.
[24] K.J.J. Steinbusch, H.V.M. Hamelers, C.M. Plugge, C.J.N. Buisman, Biological formation of caproate and caprylate from acetate: fuel and chemical production from low grade biomass, Energy Environ. Sci. 4 (2011) 216–224.
[25] H.A. Barker, M.D. Kamen, B.T. Bornstein, The synthesis of butyric and caproic acids from ethanol and acetic acid by *Clostridium Kluyveri*, Proc. Natl. Acad. Sci. U. S. A. 31 (1945) 373–381.
[26] D. Li, X. Meng, Y. Sun, X. Li, X. Liu, Z. Xie, Q. Cao, The microbial and functional reconstruction of instable syntrophic propionate-oxidizing methanogenesis by system recovering and injection modes changing, Chem. Eng. J. 455 (2023) 140736.
[27] H.C. Shin, D.-H. Ju, B.S. Jeon, O. Choi, H.W. Kim, Y. Um, D.-H. Lee, B.-I. Sang, Analysis of the microbial community in an acidic hollow-fiber membrane biofilm reactor (Hf-MBfR) used for the biological conversion of carbon dioxide to methane, PLoS One 10 (2015) e0144999.
[28] J. Subirats, H. Sharpe, E. Topp, Fate of *Clostridia* and other spore-forming Firmicute bacteria during feedstock anaerobic digestion and aerobic composting, J. Environ. Manag. 309 (2022) 114643.
[29] Q. Wu, W. Guo, X. Bao, X. Meng, R. Yin, J. Du, H. Zheng, X. Feng, H. Luo, N. Ren, Upgrading liquor-making wastewater into medium chain fatty acid: insights into co-electron donors, key microflora, and energy harvest, Water Res. 145 (2018) 650–659.
[30] S. Qiu, X. Zhang, W. Xia, Z. Li, L. Wang, Z. Chen, S. Ge, Effect of extreme pH conditions on methanogenesis: methanogen metabolism and community structure, Sci. Total Environ. 877 (2023) 162702.
[31] S.H. Zinder, Physiological ecology of methanogenesis. Methanogenesis: Ecology, Physiology, Biochemistry and Genetics, Chapman and Hall, New York, USA, 1993.
[32] J.-L. Garcia, B.K.C. Patel, B. Ollivier, Taxonomic, phylogenetic, and ecological diversity of methanogenic archaea, Anaerobe 6 (2000) 205–226.
[33] M. Liu, Y. Tang, K. Zhao, Y. Liu, X. Guo, D. Ren, W. Yao, X. Tian, Y. Gu, B. Yi, X. Zhang, Determination of the fungal community of pit mud in fermentation cellars for Chinese strong-flavor liquor, using DGGE and Illumina MiSeq sequencing, Food Res. Int. 91 (2017) 80–87.
[34] P. Louis, H.J. Flint, Diversity, metabolism and microbial ecology of butyrate-producing bacteria from the human large intestine, FEMS Microbiol. Lett. 294 (2009) 1–8.
[35] Y. Wei, Y. Wu, L. Zhang, Z. Zhou, H. Zhou, X. Yan, Genome recovery and metatranscriptomic confirmation of functional acetate-oxidizing bacteria from enriched anaerobic biogas digesters, Environ. Pollut. 265 (2020) 114843.
[36] Q. Wu, X. Bao, W. Guo, B. Wang, Y. Li, H. Luo, H. Wang, N. Ren, Medium chain carboxylic acids production from waste biomass: current advances and perspectives, Biotechnol. Adv. 37 (2019) 599–615.
[37] R. Cord-Ruwisch, H.-J. Seitz, R. Conrad, The capacity of hydrogenotrophic anaerobic bacteria to compete for traces of hydrogen depends on the redox potential of the terminal electron acceptor, Arch. Microbiol. 149 (1988) 350–357.
[38] D. Suzuki, A. Ueki, A. Amaishi, K. Ueki, *Desulfobulbus japonicus* sp. nov., a novel Gram-negative propionate-oxidizing, sulfate-reducing bacterium isolated from an estuarine sediment in Japan, Int. J. Syst. Evol. Microbiol 57 (2007) 849–855.
[39] I. Sánchez-Andrea, J.L. Sanz, M.F.M. Bijmans, A.J.M. Stams, Sulfate reduction at low pH to remediate acid mine drainage, J. Hazard. Mater. 269 (2014) 98–109.
[40] W. Shu, B. Du, G. Wu, Strategies for enriching targeted sulfate-reducing bacteria and revealing their microbial interactions in anaerobic digestion ecosystems, Water Res. 270 (2025) 122842.
[41] M.K. Nobu, T. Narihiro, C. Rinke, Y. Kamagata, S.G. Tringe, T. Woyke, W.-T. Liu, Microbial dark matter ecogenomics reveals complex synergistic networks in a methanogenic bioreactor, ISME J. 9 (2015) 1710–1722.
[42] H. Chang, B. Du, K. He, Q. Yin, G. Wu, Mechanistic understanding of acclimation and energy metabolism of acetoclastic methanogens under different substrate to microorganism ratios, Environ. Res. 252 (2024) 118911.
[43] Y. Zeng, D. Zheng, L.-P. Li, M. Wang, M. Gou, Y. Kamagata, Y.-T. Chen, K. Nobu Masaru, Y.-Q. Tang, Metabolism of novel potential syntrophic acetate-oxidizing bacteria in thermophilic methanogenic chemostats, Appl. Environ. Microbiol. 90 (2024) e01090-01023.
[44] G. Muyzer, A.J.M. Stams, The ecology and biotechnology of sulphate-reducing bacteria, Nat. Rev. Microbiol. 6 (2008) 441–454.
[45] G. Giangeri, P. Tsapekos, M. Gaspari, P. Ghofrani-Isfahani, M.K.T. Hong Lin, L. Treu, P. Kougias, S. Campanaro, I. Angelidaki, Magnetite alters the metabolic interaction between methanogens and sulfate-reducing bacteria, Environ. Sci. Technol. 57 (2023) 16399–16413.
[46] B. Du, Z. Wang, P.N.L. Lens, X. Zhan, G. Wu, New insights into syntrophic ethanol oxidation: Effects of operational modes and solids retention times, Environ. Res. 241 (2024) 117607.
[47] H.-B. Ding, G.-Y.A. Tan, J.-Y. Wang, Caproate formation in mixed-culture fermentative hydrogen production, Bioresour. Technol. 101 (2010) 9550–9559.
[48] C.M. Spirito, H. Richter, K. Rabaey, A.J.M. Stams, L.T. Angenent, Chain elongation in anaerobic reactor microbiomes to recover resources from waste, Curr. Opin. Biotechnol. 27 (2014) 115–122.
[49] L.A. Kucek, C.M. Spirito, L.T. Angenent, High n-caprylate productivities and specificities from dilute ethanol and acetate: chain elongation with microbiomes to upgrade products from syngas fermentation, Energy Environ. Sci. 9 (2016) 3482–3494.
[50] S. Cheng, Z. Liu, C. Varrone, A. Zhou, Z. He, H. Li, J. Zhang, W. Liu, X. Yue, Elucidating the microbial ecological mechanisms on the electro-fermentation of caproate production from acetate via ethanol-driven chain elongation, Environ. Res. 203 (2022) 111875.
[51] J. Xu, L. Xu, Y. Zong, R. Lin, Y. He, L. Xie, Electrically-assisted anaerobic digestion under ammonia stress: Facilitating propionate oxidation and activating methanogenesis via direct interspecies electron transfer, Bioresour. Technol. 393 (2024) 130067.
[52] B.E. Logan, R. Rossi, Aa Ragab, P.E. Saikaly, Electroactive microorganisms in bioelectrochemical systems, Nat. Rev. Microbiol. 17 (2019) 307–319.
[53] Z.M. Summers, H.E. Fogarty, C. Leang, A.E. Franks, N.S. Malvankar, D.R. Lovley, Direct exchange of electrons within aggregates of an evolved syntrophic coculture of anaerobic bacteria, Science 330 (2010) 1413–1415.